A STUDY OF BROMOETHANE PYROLYSIS

Nicolas Vin, Frédérique Battin-Leclerc, Olivier Herbinet*

Laboratoire Réactions et Génie des Procédés, CNRS, Université de Lorraine, BP 20451, 1 rue Grandville, 54000 Nancy, France.

* Corresponding author: olivier.herbinet@univ-lorraine.fr

Supplementary Description

Experimental setup

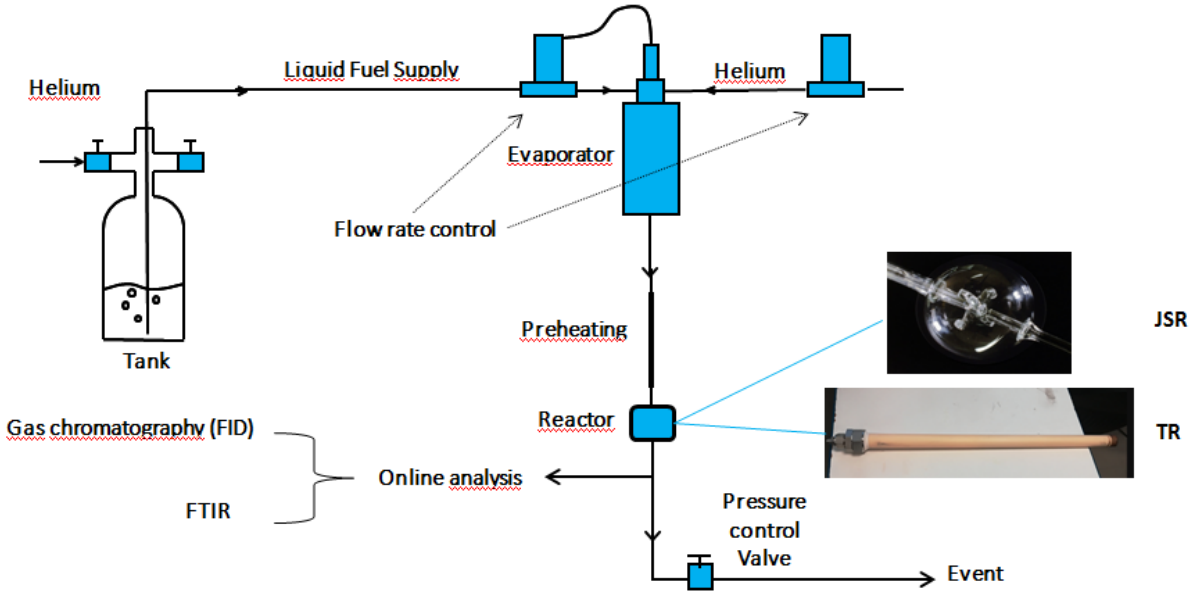

Figure S1: Scheme of the experimental setup used for running pyrolysis experiments.

Gas chromatographs (left) and GC-MS (right)

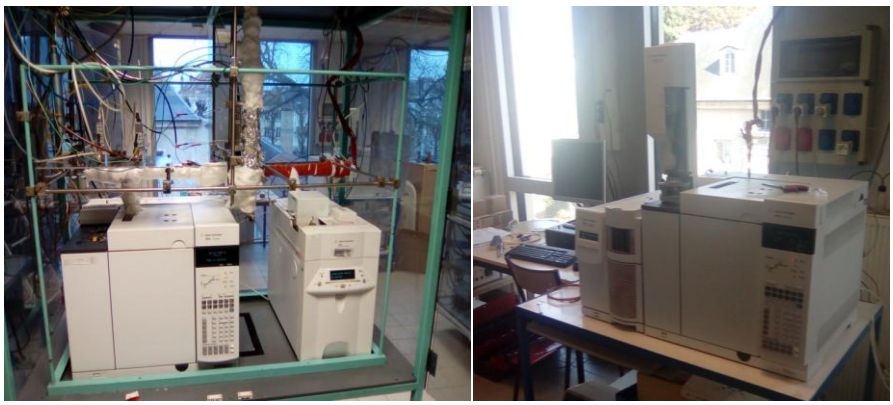

Figure S2: Pictures of gas chromatographs used for the reaction product analysis.

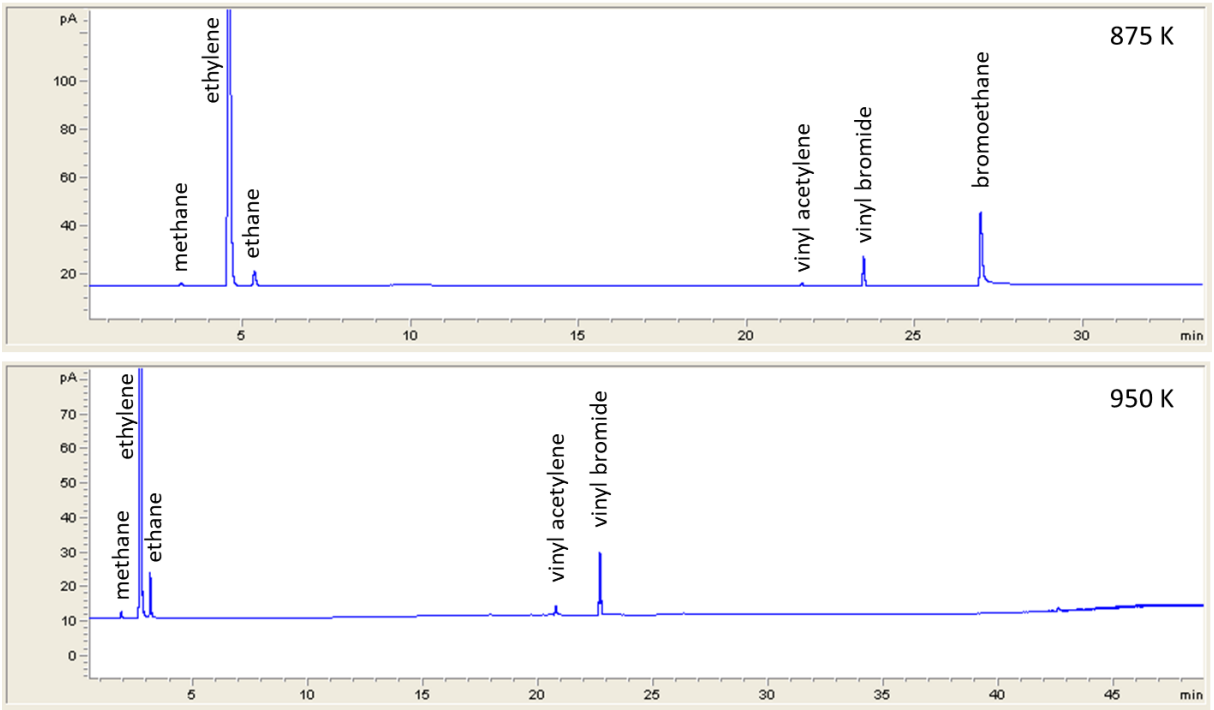

Figure S3: Two chromatograms obtained during the pyrolysis of bromoethane in a jet-stirred reactor under the conditions studied in this work (flame ionization detector, Plot-Q capillary column). See the main text for a comprehensive description of analytical conditions.

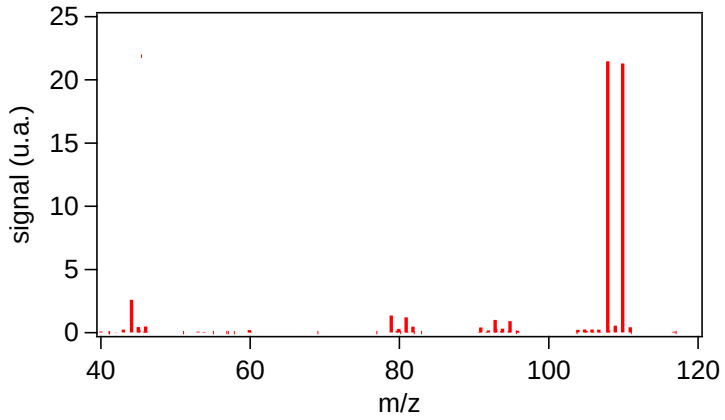

a)

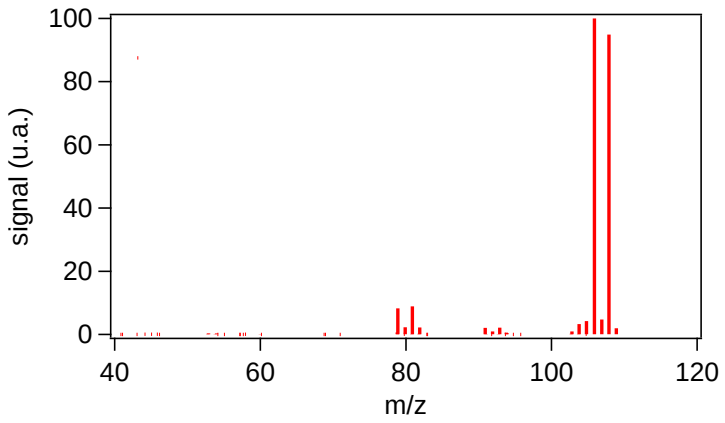

b)

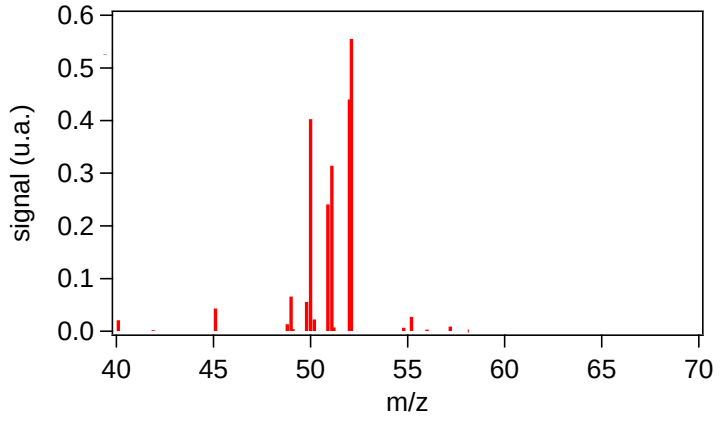

c)

Figure S4: Mass spectra recorded during experiments for the fuel (bromoethane) and for species which were not calibrated using standards. a) bromoethane, b) vinyl bromide and c) vinyl acetylene.

Residence time distribution measurements and simulations

The tubular reactor is often considered as a plug flow reactor when running simulations using detailed kinetic models. The goal of the present residence time distribution measurements and simulations is to check that this hypothesis is valid. The effect of two important parameters has been studied: the temperature and the residence time.

Experiment description

Residence time distribution measurements were performed by injecting a tracer at the inlet and recording the signal (tracer concentration) at the inlet and outlet of the reactor. The tracer used in this experiments was argon. The bath gas is helium as in combustion experiments.

The concentration of argon was measured using an online mass spectrometer (Omnistar from Pfeiffer). The sampling was achieved through a capillary tube the extremity of which was located either at the inlet, either at the outlet of the reactor.

Raw data were post-processed: the baseline was subtracted and the signal was then normalized by dividing data by the area under the signal curve.

Simulations

The simulations were performed considering that the tube is a sequence of J perfectly stirred reactors (PSR) and using the experimental inlet signal as input. The numbers of PSR was chosen so that the outlet experimental and computed profiles match. The "lsim" function[1] of the Matlab software[2] was used to compute outlet RTD profiles[1]. The transfer function used for the simulation is: $H(s) = \left(\frac{1}{1+\frac{\tau}{J}s}\right)^J$ where J is the number of PSR and τ the residence time.

Results

a) As a function of the temperature

Figure S1 shows the experimental residence time distribution (RTD) profiles measured for different temperatures (constant residence time of 2 s). The grey line is for the RTD profile recorded at the inlet of the reactor. The red dots are for the RTD profile recorded at the outlet of the reactor. The blue line is the computed RTD profile.

The shape of outlet signals is similar to that recorded at the outlet, but not exactly the same, which means that our tubular reactor is not an ideal plug flow reactor. The number of PSR J was then determined for each temperature case. $J = 105$ at 800 K, 75 at 900 K, 55 at 1000 K and 40 at 1100 K.

[1] https://www.mathworks.com/help/control/ref/lsim.html

[2] The MathWorks, Inc. et Natick, *MATLAB and Statistics Toolbox Release*. Massachusetts, United States.

It is observed that the number of PSRs decreases as the temperature increases (Figure S2). This means that the hypothesis of the plug flow reactor is less valid at high temperature than at low temperature. Nevertheless J is still equal to 40 at 1100 K, which is enough to assume that the tubular reactor behaves closely to a plug flow one. The same conclusions can be drawn from the analysis of the evolution of the values of the Peclet criterion (comparing the axial diffusion and the convection) which also decreases with the temperature (see main text).

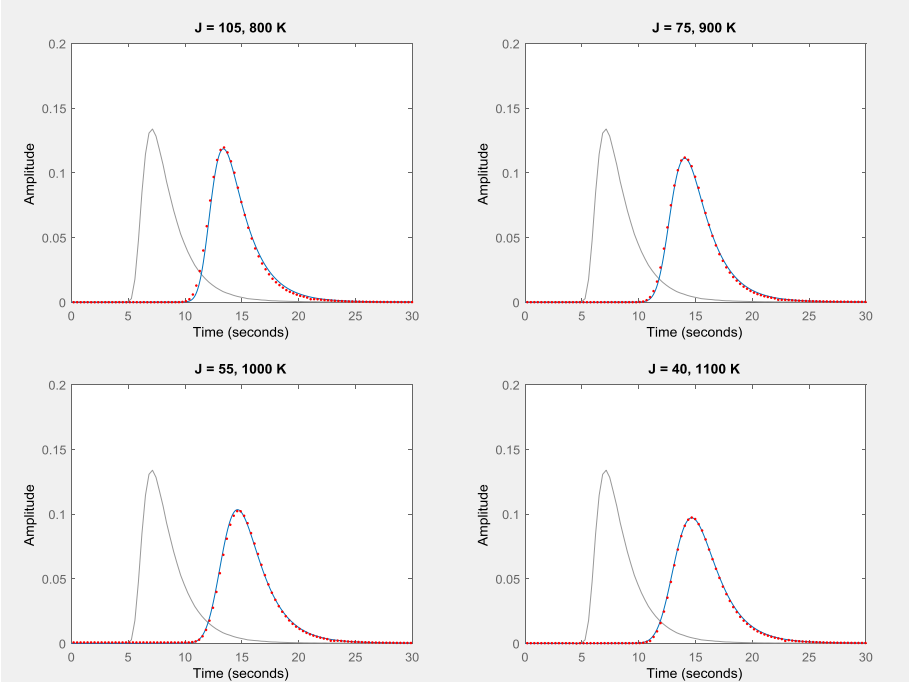

Figure S5: RTD curves for different temperatures (P = 106.7 kPa, residence time of 2 s, bath gas = helium, tracer = argon).

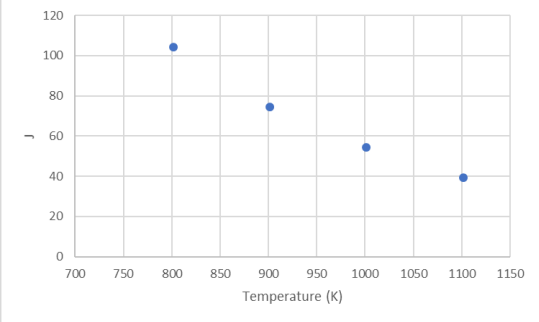

Figure S6: Evolution of J with the temperature (P = 106.7 kPa, residence time of 2 s, bath gas = helium, tracer = argon).

b) As a function of the residence time

Figure S3 shows the experimental RTD measurements performed at different residence times (2, 3, 4, 5, 6, 7 and 8 s, at the set-point temperature of 975 K) and the number J of PSRs was again determined for each case. The grey line is for the experimental inlet signal and the red dotted line is for the experimental outlet signal. The blue line is for the computed outlet signal following the same procedure as for the study of the effect of the temperature.

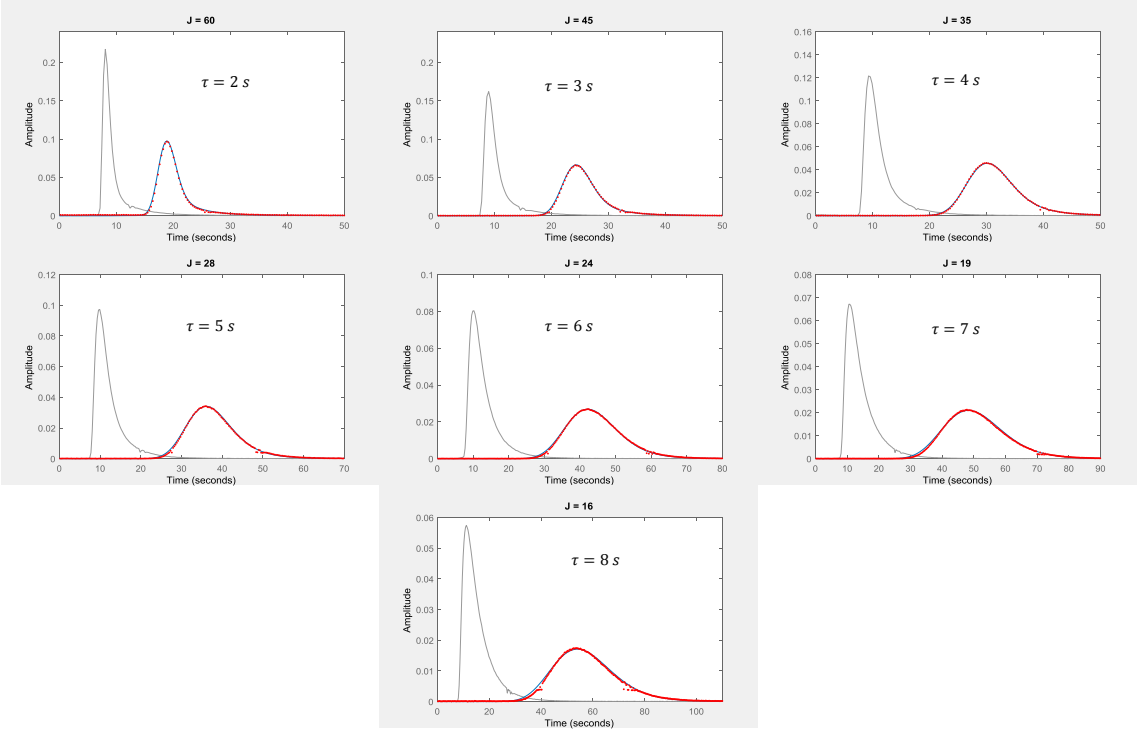

Figure S7: RTD curves for different residence times between 2 and 8 s (P = 106.7 kPa, T = 975 K, bath gas = helium, tracer = argon).

The residence time has a strong effect on the RTD as it can be seen from the distortion (enlargement) of the signal recorded at the outlet of the reactor. It can also be seen that the model does not reproduce perfectly the experimental data for long residence times, which means that the cascade of J PSR may not be the best model anymore for the tubular reactor.

The number of PSRs decreases quickly with the residence time (Figure S4): it 60 at 2 s and only 16 at 8 s. Again the hypothesis of the plug flow reactor is less valid for large residence times than for small ones. The small number of PSRs at the largest residence times can explain the deviations observed between experimental and computed data using the plug flow reactor assumption.

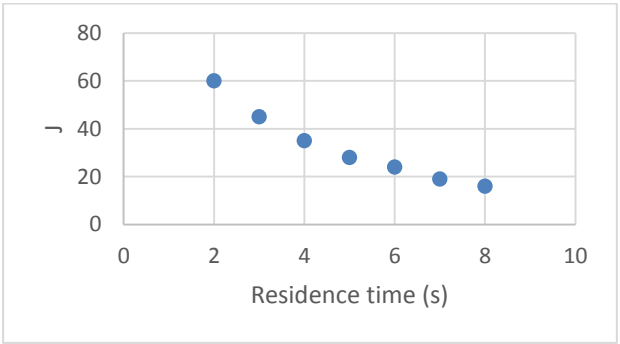

Figure S8: Evolution of J with the residence time (P = 106.7 kPa, T = 975 K, bath gas = helium, tracer = argon).

Comparison of rate calculated in this work with literature ones (when available)

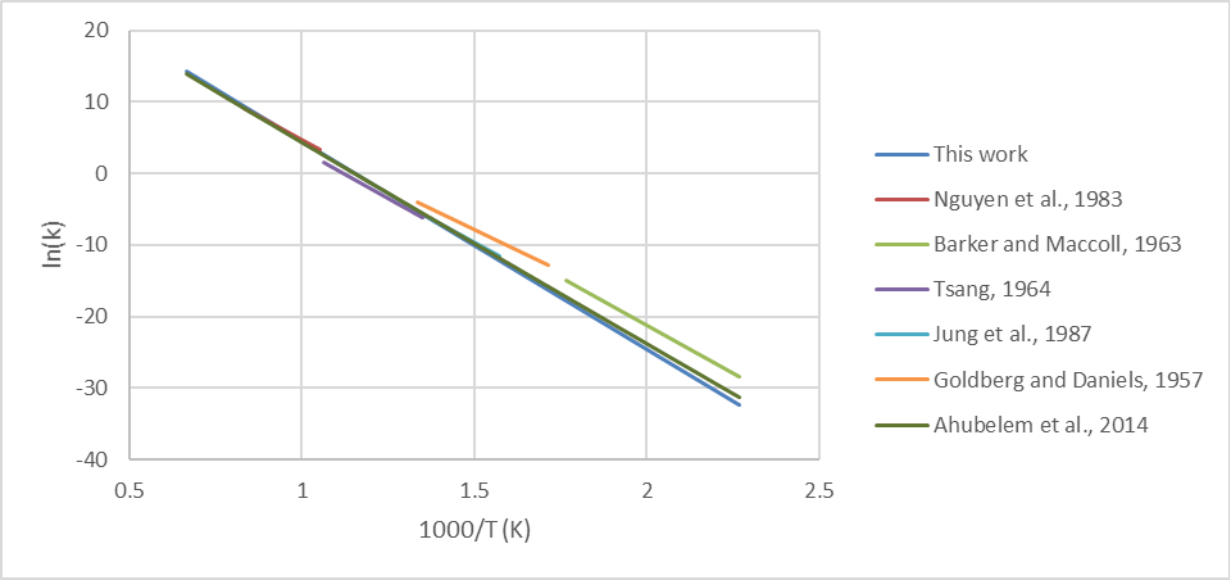

Figure S9: Comparison of literature rate constants and that calculated in this work for the molecular reaction of decomposition of C_2H_5Br to C_2H_4 and HBr.

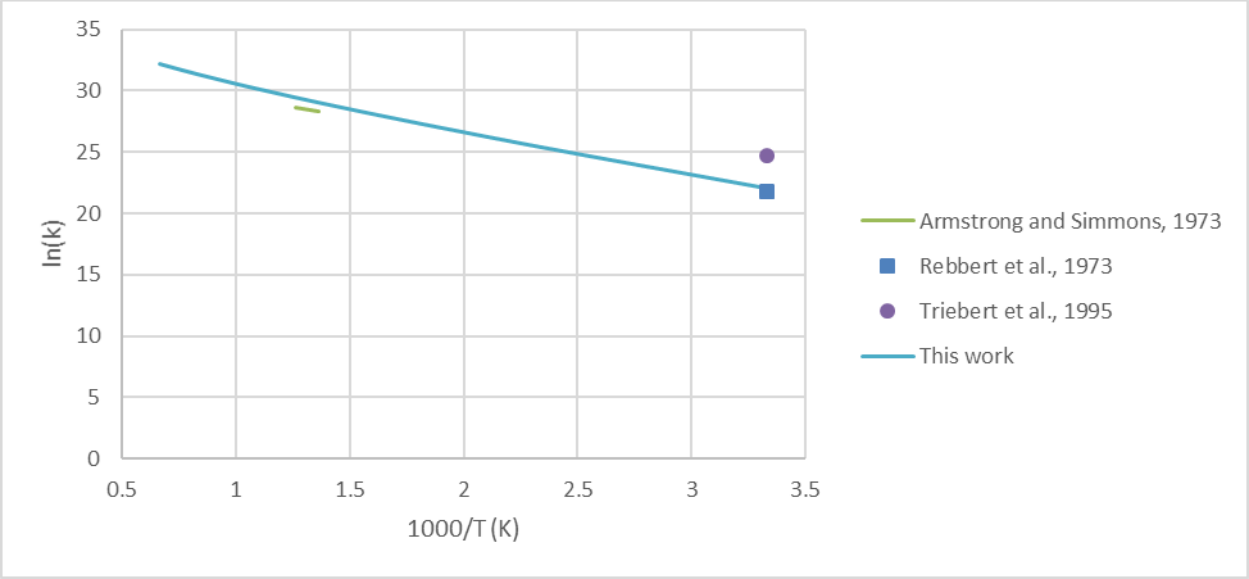

Figure S10: Comparison of literature rate constants and that calculated in this work for the reaction of Br-atom abstraction $C_2H_5Br + H$ to $C_2H_5 + HBr$.

References for Figures S9 and S10

N. Ahubelem, M. Altarawneh, B.Z. Dlugogorski, Dehydrohalogenation of ethyl halides, Tetrahedron Lett. 55 (2014) 4860–4868. doi:10.1016/j.tetlet.2014.07.009.

N. Armstrong, R.F. Simmons, Inhibition of the first limit of the hydrogen-oxygen reaction by ethyl bromide, Symposium (International) on Combustion. 14 (1973) 443–451. doi:10.1016/S0082-0784(73)80043-8.

R. Barker, A. Maccoll, Gas-Phase Photolysis of Ethyl Bromide, Journal of the Chemical Society. (1963) 2839-. doi:10.1039/jr9630002839.

A. Goldberg, F. Daniels, Kinetics of the Pyrolysis of Ethyl Bromide, J. Am. Chem. Soc. 79 (1957) 1314–1320. doi:10.1021/ja01563a018.

K. Jung, S. Kang, C. Ro, E. Tschuikowroux, Collisional Energy-Transfer in the 2-Channel Thermal Unimolecular Reaction of Bromoethane-2-D, J. Phys. Chem. 91 (1987) 2354–2358. doi:10.1021/j100293a031.

T. Nguyen, K. King, R. Gilbert, Collisional Energy-Transfer in the 2-Channel Thermal-Decomposition of Bromoethane-1,1,2,2-D4, J. Phys. Chem. 87 (1983) 494–498. doi:10.1021/j100226a024.

R. Rebbert, S. Lias, P. Ausloos, Photolysis of alkyl iodides at 147.0 nm. The reaction H + CnH2n + 1I → HI + CnH2n + 1, International Journal of Chemical Kinetics. 5 (1973) 893–908. doi:10.1002/kin.550050515.

J. Triebert, T. Meinike, M. Olzmann, K. Scherzer, On the Kinetics of Reactions of Hydrogen-Atoms with Chlorinated and Brominated Hydrocarbons, Z. Phys. Chemie-Int. J. Res. Phys. Chem. Chem. Phys. 191 (1995) 47–57. doi:10.1524/zpch.1995.191.Part_1.047.

W. Tsang, Thermal Decomposition of Some Alkyl Halides by Shock-Tube Method, J. Chem. Phys. 41 (1964) 2487-. doi:10.1063/1.1726292.

Atom balances in the tubular reactor

The deviation was calculated as follow:

$$deviation(\ in\ \%) = \frac{number\ of\ atom\ i\ at\ the\ inlet\ \ - number\ of\ atom\ i\ at\ the\ outlet}{number\ of\ atom\ i\ at\ the\ inlet} \times 100$$

Table S1: For carbon atoms:

T(K)	Deviation (%)
600	0.00
650	3.82
700	4.77
750	-2.82
775	6.73
800	8.28
825	0.49
850	1.93
875	3.63
900	-5.62
925	2.92
950	-5.81
975	2.38
Average	1.59
Standard deviation	4.31

Table S2: For bromine atoms:

T(K)	Deviation (%)
600	0.00
650	3.82
700	5.02
750	1.02
775	-0.04
800	-9.17
825	-9.18
850	-0.97
875	1.38
900	-2.03
925	4.08
950	6.88
975	1.25
Average	0.16
Standard deviation	4.84